

Characterization of a Polycrystalline Material with Laser-Excited Nonlinear Surface Acoustic Wave Pulses¹

S. N. Jerebtsov,² Al. A. Kolomenskii,²⁻⁴ and H. A. Schuessler²

High-amplitude nonlinear surface acoustic waves (SAWs) generated by laser pulses were observed in polycrystalline material (stainless steel), and the nonlinear acoustic parameters were evaluated. The velocities of bulk waves and the elastic moduli of the second order were determined by detecting the surface perturbations produced by longitudinal and shear bulk waves (precursors). Consequently, a consistent set of elastic and acoustic constants was obtained by performing all necessary measurements with the same sample using laser excitation and detection techniques.

KEY WORDS: elastic properties; laser excitation; materials characterization; nonlinear surface waves.

1. INTRODUCTION

Nonlinear properties of surface acoustic waves (SAWs) have attracted interest in different fields, in particular in materials science. The studies of the nonlinear behavior of SAWs provide data for the determination of the nonlinear elastic and acoustic constants. These constants can be used for material characterization, in particular under conditions of strong dynamic loading. In previous studies two types of the nonlinear behavior were discovered: in fused quartz [1] and fused silica [2] a nonlinear extension of

¹ Paper presented at the Fifteenth Symposium on Thermophysical Properties, June 22–27, 2003, Boulder, Colorado, U.S.A.

² Department of Physics, Texas A & M University, College Station, Texas 77843-4242, U.S.A.

³ General Physics Institute, Moscow 117942, Russia.

⁴ To whom correspondence should be addressed. E-mail: a-kolomenski@physics.tamu.edu

SAW pulses was observed, while in polycrystalline aluminum and copper a nonlinear compression of the SAW pulses was registered [2, 3]. Based on the nonlinear evolution equation [4, 5], it was shown that these differences are related to the sign of the nonlinear acoustic parameter responsible for the local nonlinearity [3]. Calculations of the nonlinear periodic SAWs in steel with the Hamiltonian approach [6, 7] have indicated the formation of a shock front for the in-plane component of the surface velocity and a sharp peak for the normal surface velocity. This behavior corresponds to a positive parameter of the local acoustic nonlinearity. An estimate of this parameter was also derived from the evolution equation [4] and shows that a positive value is expected. However, so far nonlinear acoustic parameters for stainless steel have not been determined experimentally. Therefore, in this work we present experimental and numerical results for austenitic stainless steel yielding both linear and nonlinear acoustic constants.

It should be noted that nonlinear elastic and acoustic constants of stainless steel vary drastically depending on the composition of the material. Therefore it is important to consistently measure all the parameters needed for the evaluation of the nonlinear constants in the same material. We generated high amplitude SAW pulses and observed the nonlinear changes of their shape during propagation. The surface perturbations produced by bulk waves (precursors) were used to determine the propagation velocities of the bulk waves and to calculate the second-order elastic moduli. This data allowed evaluation of the nonlinear acoustic parameters by fitting the evolution equation to experimentally measured waveforms of the nonlinear SAW pulses.

2. EXPERIMENTAL SETUP AND PROCEDURES

The SAWs were excited by nanosecond pulses of a Nd:YAG laser with a duration of 8 ns and energy up to 100 mJ. In order to maximize the opto-acoustic conversion, a thin (about 100 μm) strongly absorbing layer of fine carbon particles suspended in water or glycerine was deposited onto the surface in the excitation region. To additionally enhance the pressure acting on the surface of the sample, a glass plate with a thickness of 3 mm was placed on top of the absorbing layer. The laser radiation was sharply focused in a line of ~ 8 mm length and ~ 10 μm width near the edge of the absorption layer. This was necessary to produce the high-amplitude short SAW pulse and to avoid its strong absorption during propagation under the plate.

A sample of polycrystalline austenitic stainless steel of size 76 mm \times 76 mm \times 3 mm was used. The average grain size was about 30 μm . Although

the surface of the sample was polished to achieve better reflection, the distribution of the reflected light had still a speckle-like structure. For detection we used a calibrated probe-beam deflection setup that enabled absolute measurements of the normal surface velocity with samples exhibiting even a relatively high degree of light scattering. A SAW pulse propagated perpendicular to the excitation strip and was detected at two spots along the track as was described elsewhere [2].

The relatively low efficiency of SAW generation in polycrystalline stainless steel made the observation of nonlinear effects in this material more difficult. In addition, the high attenuation of SAWs in polycrystalline steel limited the spectrum of SAW pulses and the development of nonlinear processes. The best results were achieved by using a suspension of carbon in glycerine as an absorption liquid layer for SAW propagation distances of 5 to 14 mm from the excitation region. In order to reduce the effect of the attenuation, the thickness of the absorption layer was increased which allowed production of pulses with a longer temporal width of about 100 ns.

3. RESULTS

The SAW pulses observed for polycrystalline stainless steel at two distances are shown in Figs. 1a and b for the normal and in-plane components of the surface velocity respectively. The in-plane component was calculated from the normal component using the Hilbert transform [4]. The velocity amplitudes of the pulses were about $5 \text{ m} \cdot \text{s}^{-1}$, corresponding to an acoustic

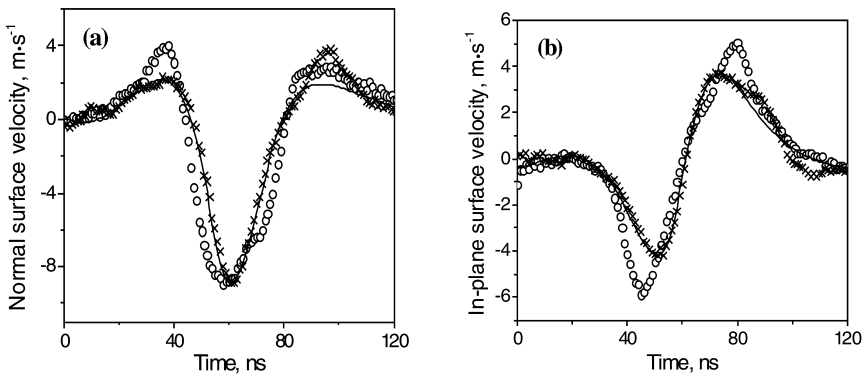


Fig. 1. SAW waveforms of the normal surface velocity registered in stainless steel at distances $x_1 = 5.2 \text{ mm}$ (open circles) and $x_2 = 16.2 \text{ mm}$ (crosses): (a) normal component, (b) in-plane component. The solid lines present the best fit calculated with $\varepsilon_1 = 4.4$, $\varepsilon_2 = -1.4$, and $\varepsilon_3 = -2.5$.

Mach number $M = 0.0017$. The comparison of the pulse forms at two propagation distances clearly shows nonlinear changes in the pulse profile. The pulse became shorter: the FWHM of the normal velocity signal was 90 ns at the second distance as compared to 120 ns at the first distance. The central part of the pulse of the in-plane component became steeper, reflecting the process of a shock front formation. Thus, a nonlinear compression of the SAW pulse took place. The amplitude of the second pulse at the second distance was less than the amplitude of the pulse at the first distance due to a strong attenuation in the polycrystalline stainless steel.

The in-plane component of the surface velocity can be described by the nonlinear evolution equation in a spectral form [4]:

$$c_R^2 \frac{\partial \bar{v}(x, \omega)}{\partial x} = \frac{(-i\omega)}{4\pi} \int_{-\infty}^{+\infty} d\omega' \bar{v}(x, \omega') \bar{v}(x, \omega - \omega') \times \left\{ \varepsilon_1 + \varepsilon_2 [1 - \text{sgn}(\omega') \text{sgn}(\omega - \omega')] + 2\varepsilon_3 \left(\frac{\omega - \omega'}{\omega} \right) \times [1 - \text{sgn}(\omega) \text{sgn}(\omega - \omega')] \right\} - \alpha_0(\omega) c_R^2 \bar{v}(x, \omega) \quad (1)$$

where $\bar{v}(x, \omega) = \int d\tau \cdot v(x, \tau) \exp(i\omega\tau)$ is the Fourier transform of the pulse profile and $\alpha(\omega)$ is the attenuation. The waveform of the nonlinear SAW pulse at the second distance was calculated using the waveform at the first distance as the initial profile. By determining the waveform with a least mean-square deviation from the experimentally measured one, the nonlinear acoustic parameters $\varepsilon_{1,2,3}$ were evaluated.

The fitting procedure was performed for five measured pairs of pulses, and the average values of the nonlinear acoustic constants were evaluated as $\varepsilon_1 = 6.0 \pm 1.7$, $\varepsilon_2 = -0.2 \pm 1.5$, and $\varepsilon_3 = -3.0 \pm 2$. The values calculated from the available data on the third-order elastic moduli for austenitic stainless steel [8] were found to be $\varepsilon_1 = 5.2$, $\varepsilon_2 = -0.04$, and $\varepsilon_3 = -3.7$.

The attenuation was determined by comparing spectral amplitudes of low-amplitude SAW pulses at two propagation distances. With the assumption that the dependence of attenuation on frequency is of the form $\alpha(\omega) = \alpha_0 \omega^2$, the attenuation coefficient α_0 was calculated as $\alpha_0 = (1/\Delta x \omega^2) \ln(A_1(\omega)/A_2(\omega))$, where $A_1(\omega)$ is the spectral amplitude of the first pulse, $A_2(\omega)$ is the spectral amplitude of the second pulse and Δx is the distance between the two probe spots. The numerical value for the attenuation coefficient was found to be $\alpha_0 \approx 1.1 \text{ m}^{-1} \cdot \text{MHz}^{-2}$.

For an elastic half space with a free boundary, a laser pulse produced simultaneously the excitation of SAWs as well as longitudinal and shear bulk waves. The surface perturbations produced by the bulk waves, labeled

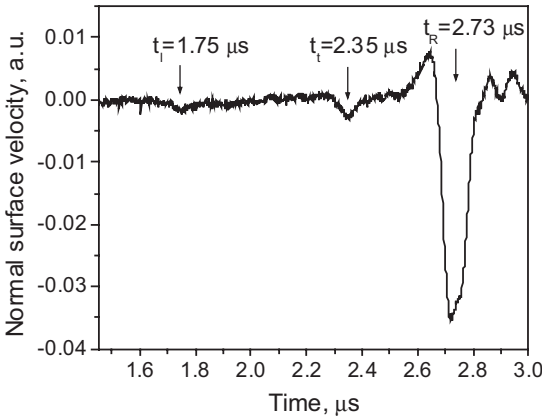


Fig. 2. Signals of surface perturbations observed on stainless steel at distance $x = 7.9$ mm. Arrival times of the longitudinal, transversal, and Rayleigh waves are indicated by vertical arrows.

precursors, were used to determine the propagation velocities of the bulk waves. The measurement of the propagation time of these waves over a known distance yielded the propagation velocities and enabled the determination of the elastic moduli of the second order. In Fig. 2 the precursors observed in stainless steel are shown. Arrivals of the longitudinal, transversal and Rayleigh waves are indicated by vertical arrows. Fused silica (Suprasil 1), as a material with well defined elastic properties and $c_R = 3430 \text{ m} \cdot \text{s}^{-1}$, was used as a reference for the determination of the propagation velocities of the longitudinal and transversal (shear) waves in stainless steel that were found to be $c_l = 4500 \text{ m} \cdot \text{s}^{-1}$, $c_t = 3300 \pm 100 \text{ m} \cdot \text{s}^{-1}$, $c_R = 2900 \pm 100 \text{ m} \cdot \text{s}^{-1}$. Using the density value $\rho = 7890 \text{ kg} \cdot \text{m}^{-3}$ measured independently, we calculated elastic moduli of the second order $c_{11} = \rho c_l^2 = 160 \pm 5 \text{ GPa}$ and $c_{44} = \rho c_t^2 = 85 \pm 3 \text{ GPa}$.

4. DISCUSSION

The observed nonlinear transformation of SAW pulses in polycrystalline stainless steel has some special features as compared to similar effects observed previously in polycrystalline aluminum and copper [2, 3]. The parameter of the local nonlinearity ε_1 is larger in polycrystalline stainless steel than in the two other metals. However, with the same generation mechanism, SAW pulses with significantly lower amplitudes were generated in stainless steel. Thus, the relatively weaker manifestation

of the nonlinearity in stainless steel as compared to aluminum is connected to the considerably lower values of the amplitude of the generated SAW pulses (by a factor of about three) occurring in the experiments with steel. A common feature observed in all polycrystalline metals investigated so far is the positive nonlinear acoustic parameter ε_1 , which results in the nonlinear compression of SAW pulses. This may indicate that the nature of the acoustic nonlinearity is related to the polycrystalline structure of these materials.

The deviations of the experimental and theoretical values for $\varepsilon_{1,2}$ can be attributed to individual variations of the material composition. The larger scatter of values for ε_3 is due to the fact that the pulse shape is relatively insensitive to the variations of this parameter. Another possible explanation is the influence of the microplasticity and hysteresis effect in polycrystalline materials [10], which was not taken into account in the theoretical model used.

ACKNOWLEDGMENTS

This material is based upon work supported by the National Science Foundation under Grants No. 9870143 and 9970241.

REFERENCES

1. A. A. Kolomenskii, A. M. Lomonosov, R. Kuschnerit, P. Hess, and V. E. Gusev, *Phys. Rev. Lett.* **79**:1325 (1997).
2. A. A. Kolomenskii and H. A. Schuessler, *Phys. Rev. B* **63**:85413 (2001).
3. A. A. Kolomenskii and H. A. Schuessler, *Phys. Lett. A* **280**:157 (2001).
4. V. E. Gusev, W. Lauriks, and J. Thoen, *Phys. Rev. B* **55**:9344 (1997).
5. V. E. Gusev, W. Lauriks, and J. Thoen, *J. Acoust. Soc. Am.* **103**:3203 (1998).
6. E. A. Zabolotskaya, *J. Acoust. Soc. Am.* **91**:2569 (1992).
7. M. F. Hamilton, Y. A. Il'inskii, and E. A. Zabolotskaya, *J. Acoust. Soc. Am.* **105**:639 (1999).
8. Landolt-Börnstein, *Numerical Data and Functional Relationships in Science and Technology* (Springer, Heidelberg, 1984), New Series, Group 3, Vol. 11.
9. A. A. Kolomenskii and A. A. Maznev, *Sov. Phys. Acoust* **36**:258 (1990).
10. V. E. Nazarov, L. A. Ostrovskii, I. A. Soustova, and A. M. Sutin, *Sov. Phys. Acoust.* **34**:284 (1988).